Trends of ocean acidification and pCO2 in the Northern North Sea, 2003–2015

Abdirahman M. Omar, H. Thomas, Are Olsen, Meike Becker, Ingunn Skjelvan, Gilles Reverdin

JGR Biogeosciences

RESEARCH ARTICLE
10.1029/2018JG004992

Trends of Ocean Acidification and pCO_2 in the Northern North Sea, 2003–2015

A. M. Omar[1], H. Thomas[2], A. Olsen[3], M. Becker[3], I. Skjelvan[1], and G. Reverdin[4]

[1]Norwegian Research Centre AS, Bjerknes Centre for Climate Research, Bergen, Norway, [2]Institute of Coastal Research, Helmholtz Center Geesthacht, Geesthacht, Germany, [3]Geophysical InstituteUniversity of Bergen, Bjerknes Centre for Climate Research, Bergen, Norway, [4]Sorbonne-Université, CNRS/IRD/MNHN (LOCEAN), Paris, France

Abstract For continental shelf regions, the long-term trend in sea surface carbon dioxide (CO_2) partial pressure (pCO_2) and rates of ocean acidification are not accurately known. Here, we investigate the decadal trend of observed wintertime pCO_2 as well as computed wintertime pH and aragonite saturation state (Ω_{ar}) in the northern North Sea, using the first decade long monthly underway data from a voluntary observing ship covering the period 2004–2015. We also evaluate how seawater CO_2 chemistry, in response to physical and biological processes, drives variations in the above parameters on seasonal and interannual timescales.

In the northern North Sea, pCO_2, pH, and Ω_{ar} are subject to strong seasonal variations with mean wintertime values of 375 ± 11 μatm, 8.17 ± 0.01, and 1.96 ± 0.05. Dissolved inorganic carbon is found to be the primary driver of both seasonal and interannual changes while total alkalinity and sea surface temperature have secondary effects that reduce the changes produced by dissolved inorganic carbon. Average interannual variations during winter are around 3%, 0.1%, and 2% for pCO_2, pH, and Ω_{ar}, respectively and slightly larger in the eastern part of the study area (Skagerrak region) than in the western part (North Atlantic Water region). Statistically significant long-term trends were found only in the North Atlantic Water region with mean annual rates of 2.39 ± 0.58 μatm/year, −0.0024 ± 0.001 $year^{-1}$, and −0.010 ± 0.003 $year^{-1}$ for pCO_2, pH, and Ω_{ar}, respectively. The drivers of the observed trends as well as reasons for the lack of statistically significant trends in the Skagerrak region are discussed.

Plain Language Summary Temperate and high latitude marine shelf areas are generally net sinks of atmospheric carbon dioxide (CO_2), and they are experiencing ocean acidification. Decadal trends in the magnitude of the sinks and acidification occurring in these regions are not accurately known mainly due to limited time series and higher natural spatiotemporal variability compared to open oceans. Hence, an important question is whether the surface seawater CO_2 growth and acidification on the shelves can be predicted from atmospheric CO_2 increase as is the case for the open oceans? To contribute to the answer of this question, we compiled the first decade-long, monthly time series of surface seawater CO_2 and acidification parameters in the northern North Sea (2004–2015). Our analyses confirm that the area is a year-round CO_2 sink and further demonstrate its strong seasonal and interannual variations. In the western parts of the study area, we found wintertime trends that are statistically significant and similar to what is expected from atmospheric CO_2 increase and observed in the open ocean. In the eastern parts, seasonal and interannual changes were somewhat stronger, but wintertime trends were weaker and not statistically significant.

Key Points:
- The study area is a year-round CO_2 sink with strong seasonal and spatial variations
- DIC is the primary driver of variability in pCO_2 and ocean acidification variables while SST and TA have couteracting secondary influences
- In the western region, rates of pCO_2 growth and acidification over the last decade closely tracked the atmospheric CO_2 increase

Supporting Information:
- Supporting Information S1

Correspondence to:
A. M. Omar,
abdir.omar@uni.no

Citation:
Omar, A. M., Thomas, H., Olsen, A., Becker, M., Skjelvan, I., & Reverdin, G. (2019). Trends of ocean acidification and pCO_2 in the northern North Sea, 2003–2015. *Journal of Geophysical Research: Biogeosciences*, *124*, 3088–3103. https://doi.org/10.1029/2018JG004992

Received 17 DEC 2018
Accepted 23 AUG 2019
Accepted article online 16 SEP 2019
Published online 29 OCT 2019

1. Introduction

The increase in the atmospheric carbon dioxide (CO_2) concentration drives anthropogenic net ocean CO_2 uptake and this leads to ocean acidification (OA, e.g., Royal Society, 2005). OA is currently receiving an intensive research attention because of its negative effects on many marine organisms including decreased survival, calcification, growth, development, and abundance (Kroeker et al., 2013).

The rates of OA vary between ocean regions. For the open ocean, where uptake of anthropogenic CO_2 from the atmosphere is the dominant driver, the OA rate over the last decades has been relatively well documented and understood (e.g., Bates et al., 2014). Observations from time series stations and volunteer observing ships (VOS) in different oceanic regions consistently show systematic changes in surface ocean chemistry

resulting from OA. Specifically, long-term negative trends of pH and aragonite saturation state (Ω_{ar}) have been observed (e.g., Bates et al., 2014; Lauvset et al., 2015).

For coastal regions, observed rates of pH change differ from those expected from oceanic CO_2 uptake alone, as changes in other biogeochemical processes, related for example to changes in nutrient loading and eutrophication, are important as well (Burt et al., 2016; Cai et al., 2017; Clargo et al., 2015; Provoost et al., 2010; Wootton et al., 2008). Moreover, the long-term trend in atmosphere-ocean pCO_2 difference, the thermodynamic force of the CO_2 uptake from the atmosphere, is not accurately known for shelf regions. For instance, Wang et al. (2017) reported that in Northern Hemisphere marginal seas, the rate of change of surface ocean pCO_2 on decadal time scales (1.9 $\pm$ 1.6 μatm/yearr) closely follows the rate of atmospheric pCO_2 increase (1.90 $\pm$ 0.06 μatm/year), that is, the atmosphere-ocean difference is constant. Laruelle et al. (2018), on the other hand, used global data spanning a period of up to 35 years and found a tendency of increased uptake, that is, a seawater pCO_2 growth rate that lagged that in the atmosphere, in 80% of the investigated shelf regions for which a trend could be calculated. They also pointed out that trends appear highly variable both within the same shelf and across different shelf systems.

The North Sea is one of the best-studied shelf seas with respect to carbon cycle biogeochemistry (Bozec et al., 2005, 2006; Omar et al., 2010; Thomas et al., 2004, 2005, 2007). In the seasonally stratified northern North Sea, including the western Norwegian fjords, carbon is taken up by phytoplankton in the surface and respired in the subsurface layer (Thomas et al., 2004). The area is undersaturated with respect to atmospheric CO_2 throughout the year, driving a flux of CO_2 into the ocean (Omar et al., 2010; Omar et al., 2016). There are also large seasonal variations, driven by biology and mixing, temperature changes, and air-sea CO_2 exchange. The hydrography and biogeochemical properties of the northern North Sea are mainly influenced by two water inflows (e.g., Chierichi et al., 2017; Lee, 1980). In the eastern parts (east of 6°E), high input of less saline water from the Baltic Sea and from the Norwegian coast occurs and the low salinity (S) Skagerrak water (SW) flows northward along the Norwegian coast. In the western parts, the warm saline North Atlantic Water (NAW) enters from the north-west opening and extends as far south as about 55°N where during summer, it is overlain by a combination of fresher coastal water and/or SW. These regions will be henceforth referred to as the Skagerrak and NAW regions, respectively.

Interannual variations are significant in the North Sea, and their magnitude appears to be dependent on region and season, being generally enhanced in the southern North Sea and during summer/spring (Omar et al., 2010). Salt et al. (2013) reported that the North Atlantic Oscillation index influences the CO_2 system in the North Sea by regulating the inflow of water from North Atlantic and Baltic. During positive North Atlantic Oscillation index, higher rates of the above inflows lead to a limited mixing between the north and south, and this leads to a steeper gradient in pH and pCO_2 between south and north in the productive period.

The long-term trends are poorly quantified due to lack of proper long-term time series, but published low resolution repeated measurements indicate that the increase in atmospheric pCO_2 is driving a secular increase in surface water pCO_2 in the North Sea (Clargo et al., 2015; Omar et al., 2010; Thomas et al., 2007). However, observation-based OA estimates and studies considering decadal trends are still scarce.

Here, we investigate the decadal trend of wintertime pCO_2 as well as pH and Ω_{ar} in the northern North Sea for the period 2004–2015. We combine the underway data from a VOS with available multiyear, basin-wide station data from research cruises to facilitate a complete description of the seawater CO_2 chemistry as was described in Lauvset et al. (2015). We focus on analyses of pCO_2, Ω_{ar}, and pH values and evaluate their spatiotemporal variations and drivers. First, we present the mean distribution along the track of the VOS line to understand the seasonal and spatial patterns. Then we divide the data into NAW and Skagerrak regions to analyze interannual and long-term changes and their drivers. The long-term changes are determined during the winter season when the influence of biological activity is minimal and the computed trends are compared to those observed in the adjacent open ocean regions.

2. Material and Methods

2.1. Monthly Underway VOS Data

Underway measurements of sea surface pCO_2 and temperature (SST) were obtained on the containership M/V Nuka Arctica (henceforth Nuka; operated by Royal Arctic Line, www.ral.dk,nuka.uib.no). Nuka

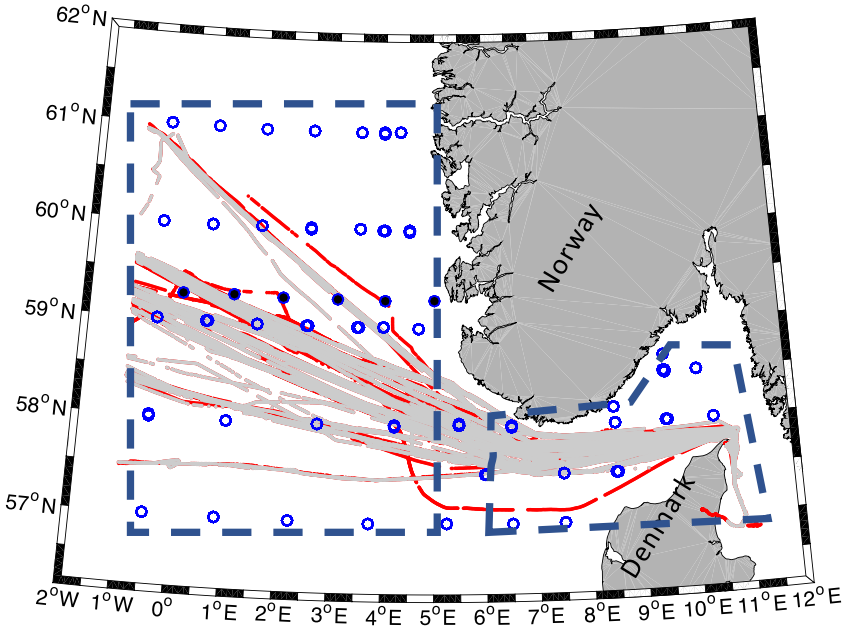

Figure 1. Map of the northern North Sea showing the tracks of the containership Nuka Arctica (red dots) overlaid by tracks for which satellite derived net primary productivity has been collocated with the ship measurements (gray dots). Also shown are stations covered during the cruises aboard R/V Pelagia (blue circles: 2005, 2008, and 2011) and R/V GO Sars (blue filled circles: 2015). The region enclosed by the dashed rectangle is referred to as the North Atlantic Water region whereas the region enclosed by the polygon is referred to as the Skagerrak region in the main text.

crosses the North Sea approximately every 3 weeks along a transect between 59.5–57.7°N heading southeast until 7°E, and then continues eastward until 10°E, where it turns southward before entering the port of Aalborg, Denmark (Figure 1). The measurement system was installed on Nuka in 2004. It was first installed in the bow thruster room, but was relocated in early 2006 to the engine room close to the middle of the ship, in order to reduce the amount of air bubbles in the seawater stream. The pCO_2 measurements on Nuka were first presented in Olsen et al. (2008) and are conducted using an instrument based on the design and recommendations of Pierrot et al. (2009). Briefly, the instrument uses a nondispersive infrared CO_2/H_2O gas analyzer (LI-COR 6262) to determine the CO_2 concentration in headspace air in equilibrium with a continuous stream of seawater. Headspace analyses are carried out every minute, and the instrument is calibrated roughly every 6 hr with three reference gasses, which are traceable to reference standards provided by National Oceanic and Atmospheric Administration/Earth System Research Laboratory. The LI-COR is calibrated approximately three times per day using N_2 ($CO_2 = 0$) and the standard gas with the highest CO_2 concentration. Data acquired between 57°N–61°N and 1.0°W–10.4°E are used for the analyses in this contribution. They were extracted from the SOCATv6 database (Bakker et al., 2014). The accuracy of the pCO_2 instrument on Nuka is approximately ±2 μatm.

Sea surface S (SSS) data are measured on Nuka using a SBE-21 Seacat thermosalinograph. The data are calibrated following Alory et al. (2015), excluding data that are indicative of insufficient water flow rates. The remaining data are corrected based on in situ water samples, collected across the Atlantic and analyzed at the Grønland Naturinstitut, Nuuk, Greenland, and occasional close-by Argo data with quality flags "good." Corrections are typically in the range of 0 to 0.6 psu.

2.2. Cruise Data

We supplemented the VOS data with station data acquired during four scientific cruises in the study area in the period 2005–2015. Three of these were late summer cruises conducted in the North Sea on R/V Pelagia on (17 August 2005–5 September 2005; 21 August 2008–7 September 2008; 1–25 September 2011). These data have been described in detail by Thomas et al. (2007), Bozec et al. (2005), Thomas et al. (2004), and Thomas (2002). Briefly, the Pelagia cruises covered the North Sea during all four seasons and obtained

station data with a sampling resolution of approximately 1° by 1°. During each cruise, water column profile data for (but not limited to) dissolved inorganic carbon (DIC), total alkalinity (TA), S, and temperature were obtained. DIC and TA have been determined using the coulometric method according to Johnson et al. (1993) and a Gran potentiometric open cell titration, respectively. Uncertainty was 1–2 μmol/kg (≈0.8‰) for DIC and 2–3 μmol/kg (≈1‰) for TA. The 2005 and 2008 cruise data have been released as part of the GLODAPv2 data synthesis (Olsen et al., 2016). Similar water column carbonate measurements were also carried out in April 2015 on R/V GO Sars (Fröb et al., 2019). The 2015 cruise covered an east-west section perpendicular to the Norwegian west coast (59.3°N, 3–4°E; Figure 1, blue filled circles) and the data are available at https://cchdo.ucsd.edu/cruise/58GS20150410.

2.3. Satellite Derived Productivity Data

Monthly values for net primary production (NPP), based on the standard Vertical General Production Model which uses MODIS surface chlorophyll, SST, and photosynthetically active radiation (Behrenfeld & Falkowski, 1997) have been downloaded from the Oregon State University Ocean Productivity website. Negative values have been filtered out, and a subset of the data has been colocated with the data from Nuka (Figure 1).

2.4. Complete Description of the Seawater CO_2 System

To obtain a complete description of the seawater CO_2 system from the underway SST and pCO_2 data collected on Nuka, we used the frequently applied empirical approach that has been described in the literature (Lauvset et al., 2015; Nondal et al., 2009; Omar et al., 2010; Takahashi et al., 2014). The approach takes advantage of the strong correlation between TA and S in the ocean, which can be described with an empirical linear relationship of the form $TA = a \times S + b$. Here, we used the cruise data sets to identify separate TA-S relationships, one from each cruise data set. The available cruise data were not sufficient to study seasonal changes in TA-S regressions in detail but was suitable to assess the interannual variability. Therefore, we derive separate TA-S relationships in order to be able to assess any interannual variations in the coefficients for the regressions and their significance for the computations (section 3.1). Furthermore, we have chosen to use full depth profile data (not only surface data) for the regressions because the North Sea is well mixed during winter (e.g., Thomas et al., 2004). Therefore we assume that data from deepest parts of the water column are representatives for winter conditions. The robustness of this assumption is tested during the validation of the TA-S regression (below). Moreover, the regression coefficients from the 2005 cruise were applied to the underway S data to compute TA values for 2004, 2005, and 2006; the coefficients from the 2008 cruise were used for computing TA values in 2007, 2008, and 2009; the coefficients from the 2011 cruise were used for TA values in 2010, 2011, and 2012; and finally, the coefficients from the 2015 cruise were used for TA values in 2013, 2014, and 2015.

The seawater CO_2 chemistry was fully described with the measured pCO_2 and the TA derived from S, using the dissociation constants of Millero et al. (2006) as implemented in CO2SYS (Lewis & Wallace, 1998; van Heuven et al., 2011). This choice of constants follows the recommendation of Salt et al. (2015), who investigated the internal consistency of the North Sea carbonate system. The KSO_4 dissociation constant of Dickson (1990) has been used and nutrient concentrations were set to zero during the above calculations. pH was determined on the total scale.

The TA-S relationship and the pH, DIC, and Ω_{ar} values estimated from calculated TA and pCO_2, were validated using TA measurements and pH and Ω_{ar} values computed from TA and DIC as measured on RV Pelagia cruises in November 2001 and February 2002, which has been described in Thomas et al. (2004). The 2001–2002 cruise data have not been used for deriving the TA-S relationships and so are fully independent. Furthermore, these winter data gave us a perfect opportunity to test the assumption that our TA-S relationship is valid for winter data since our regression coefficients were identified using profile data including subsurface samples with concentrations that resemble wintertime concentrations at the surface (2,214–2,339 μmol/kg). Thus, for the validation purpose, we disregarded the effect of interannual changes in the TA-S relationships (section 3.1) which is minimal during winter, and we used the mean values of the regression coefficients. The residuals (measured/computed-predicted) for TA, pH, DIC, and Ω_{ar} are shown in Figure S1 in the supporting information, and mean differences were -12.5 ± 9.3 μmol/kg for TA, -0.002 ± 0.002 for pH, -11 ± 8 μmol/kg for DIC, and -0.02 ± 0.02 for Ω_{ar}. Slightly higher residuals

Table 1
Coefficients for TA Versus S Regressions and Associated Statistics During Different Cruises

Cruise time (month, year)	Slope (μmol/kg)	Intercept (μmol/kg)	R^2	p	#n	RMSE (μmol/kg)
Aug–Sep 2005	25.1 ± 0.4	1,438 ± 13	0.92	<0.005	392	7
Aug–Sep 2008	25.4 ± 0.4	1,432 ± 14	0.91	<0.005	379	8.9
Sep 2011	24.9 ± 0.4	1,447 ± 12	0.92	<0.005	425	7
May 2015	28.0 ± 0.8	1,339 ± 29	0.98	<0.005	30	3

Note. RMSE = root mean square error; S = salinity; TA = total alkalinity.

for midrange TA in the 2001 data (and corresponding increased residuals in lowest DIC and highest pH and Ω_{ar} values) were observed and probably were due to the aforementioned interannual variations in the TA-S relationship. By combining the maximum mean difference obtained from above residuals and typical uncertainties in pH values calculated from DIC-TA pairs (e.g., Omar et al., 2016), we estimated the total error associated with our computed pH and Ω_{ar} values to be ±0.01 and ±0.1, respectively. For TA and DIC, we will use a total error of ±16 μmol/kg and ±19 μmol/kg which we obtained by combining the mean offsets (13 and 11 μmol/kg) and the random errors (±9.3 and ±8 μmol/kg), respectively.

3. Results and Discussion

3.1. Identified Empirical Relationships

The relationships between TA and S obtained from the cruise data from 2005, 2008, 2011, and 2015 are presented in Table 1. Statistically significant ($R^2 > 0.9$ and $p < 0.001$) positive linear relationships were found with maximum root mean square error values that were within 3 times the state-of-the-art measurement uncertainty (2–3 μmol/kg, Dickson, 2010). The slopes and intercepts of the regression equations ($y = ax + b$) varied between the different years with mean and standard deviation values of $a = 25.9 \pm 1.4$ μmol/kg and $b = 1{,}414 \pm 50$ μmol/kg, respectively. The high intercept values indicate the presence of substantial inorganic carbon in the freshwater component (e.g., Olsson & Anderson, 1997) and are in agreement with earlier results from the area. Omar et al. (2010) reported an intercept of 1,817 ± 48 μmol/kg based on data from 2001 and 2002. Salt et al. (2013) investigated the effect of variable mixing between North Sea and SW by using data obtained in 2001, 2005, and 2008, and considering samples containing >3% of Baltic water mass fraction. They reported slopes and intercepts ranging between 20–27 μmol/kg and 1,390–1,590 μmol/kg, respectively, and argued that the interannual variability in the slopes and intercepts largely reflects changes in the water mass fractions rather than changes in the end-member concentrations. Despite the significant differences in the regression coefficients (Table 1), TA values predicted by the four regression equations were in agreement with each other to within total uncertainty of ±16 μmol/kg. Thus, sensitivity analyses showed that all the results presented in the subsequent sections could also be obtained by using the mean values of the coefficients. This means that the identified variability in the coefficients is not significant enough to impact our main findings.

3.2. Seasonal and Spatial Patterns Along the Ship Track

Clear seasonal variations are observed in all variables; SST, NPP, pH, and Ω_{ar} all increase from winter to summer, while SSS and pCO_2 decrease (Figure 2). The patterns and magnitudes of the seasonal variations are similar to those reported earlier for the area (e.g., Omar et al., 2010; Salt et al., 2015; Thomas et al., 2005). The seasonal change in SST exceeds 10 °C, with coldest SST in February and March and warmest SST in August (Figure 2a). Furthermore, during winter and early spring, SST decreases eastward, but from late spring through fall the spatial SST gradient reverses as a result of decreased mixed layer throughout the study area combined with solar radiation input that increases eastward in the northern North Sea (Otto et al., 1990).

The spatial variations of SSS show the main water masses in the study area: the saline NAW (SSS > = 35) is usually encountered in the western part of the transect (west of 5°E; i.e., in the NAW region; Figure 2b) and the fresher SW in the east (east of 6°E; i.e., in the Skagerrak region). Seasonal variations are stronger in the Skagerrak region, being fresher (SSS < 31) during summer (July) and more saline (SSS > 33) during winter (January). In the NAW region, SSS values of 34 appear between May and August.

pCO_2 is highest (360–400 μatm) during late fall (November) and early winter (December–January) and lowest (<280 μatm) during spring (March–May; Figure 2c). Furthermore, the low values during spring appear first in the eastern side of the study area and propagate westward while the increase of pCO_2 toward maximum winter values propagates eastward, except in the area east of 9°E, where pCO_2 values >300 μatm appear already in July. The high wintertime pCO_2 values stayed around the concurrent atmospheric pCO_2 values obtained at Mace Head, Ireland, (Bousquet et al., 1996) throughout the study period (Figure S2).

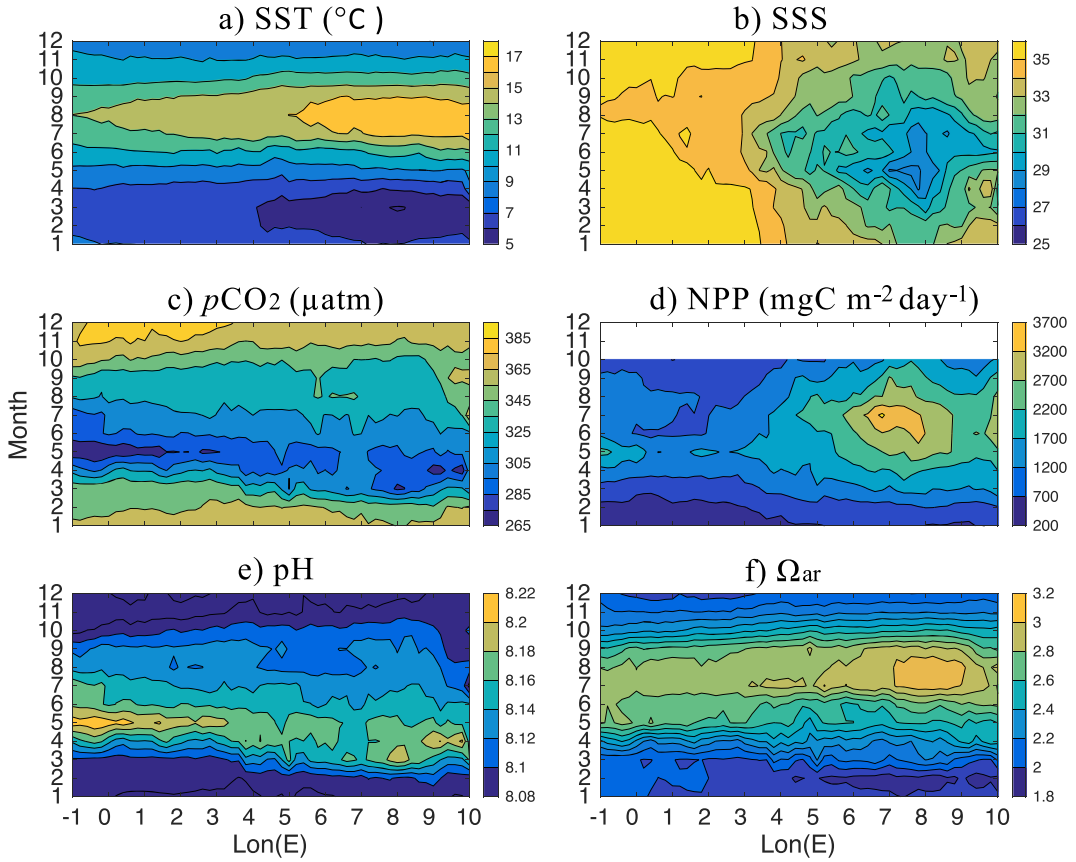

Figure 2. (a) SST, (b) SSS, (c) pCO_2, (d) satellite derived NPP, (e) computed pH, (f) computed Ω_{ar}, as a function of longitude and month of the year. All data from 2004–2014 have been condensed into one virtual year and bin-averaged into 0.2 longitudes to resolve the spatial and seasonal variations. NPP = net primary production; SSS = sea surface salinity; SST = sea surface temperature.

This confirms that the area is a year-round sink for atmospheric CO_2 (Omar et al., 2010). The decrease during spring is due to biological carbon uptake by the spring phytoplankton bloom (Frankignoulle & Borges, 2001; Thomas et al., 2004). During the rest of the year, thermodynamic, remineralization, and mixing processes mainly control pCO_2 (these controls are quantified below).

The satellite derived NPP is high (>1,000 mg C·m^{-2}·day^{-1}) between April and October with the most intense and longest bloom periods occurring in areas close to land (Figure 2d), that is, south of Norway (Figure 1). For instance, in the Skagerrak region, NPP > =2,000 mg C·m^{-2}·day^{-1} between April and October whereas further offshore, in the central northern North Sea, NPP reaches >1,000 mg C·m^{-2}·day^{-1} only in April–August. Furthermore, significant NPP occurs in the Skagerrak region even as early as March. If integrated over the whole year, the typically annual NPP values are around 200 g C/m^2 for the NAW region and 500 g C/m^2 for the Skagerrak region. However, for both regions, the estimated values are probably highly overestimated since the VGPM model has been shown to overestimate NPP in the North Atlantic by 100% due to high sensitivity to variations in temperature (e.g., Tilstone et al., 2015). In fact, model results of Moll (1997) reported annual NPP values of 100–125 g C·m^2·year^{-1} and 125–200 g C·m^2·year^{-1} in the NAW and Skagerrak regions, respectively (his Figure 3) which are about 100% lower than the above estimated annual NPP values.

The spatial and seasonal patterns of the estimated pH are opposite to those observed in pCO_2, reflecting the close inverse relationship between these two variables. pH is lowest (8.05–8.08) during late fall and winter and highest (>8.15) during spring (Figure 2e).

The mean distribution of Ω_{ar} also shows a significant seasonal variation (Figure 2f). A notable feature is that the maximum Ω_{ar} (>2.5) occurs 1–2 months after the maximum pH and minimum pCO_2 (compare Figure 2

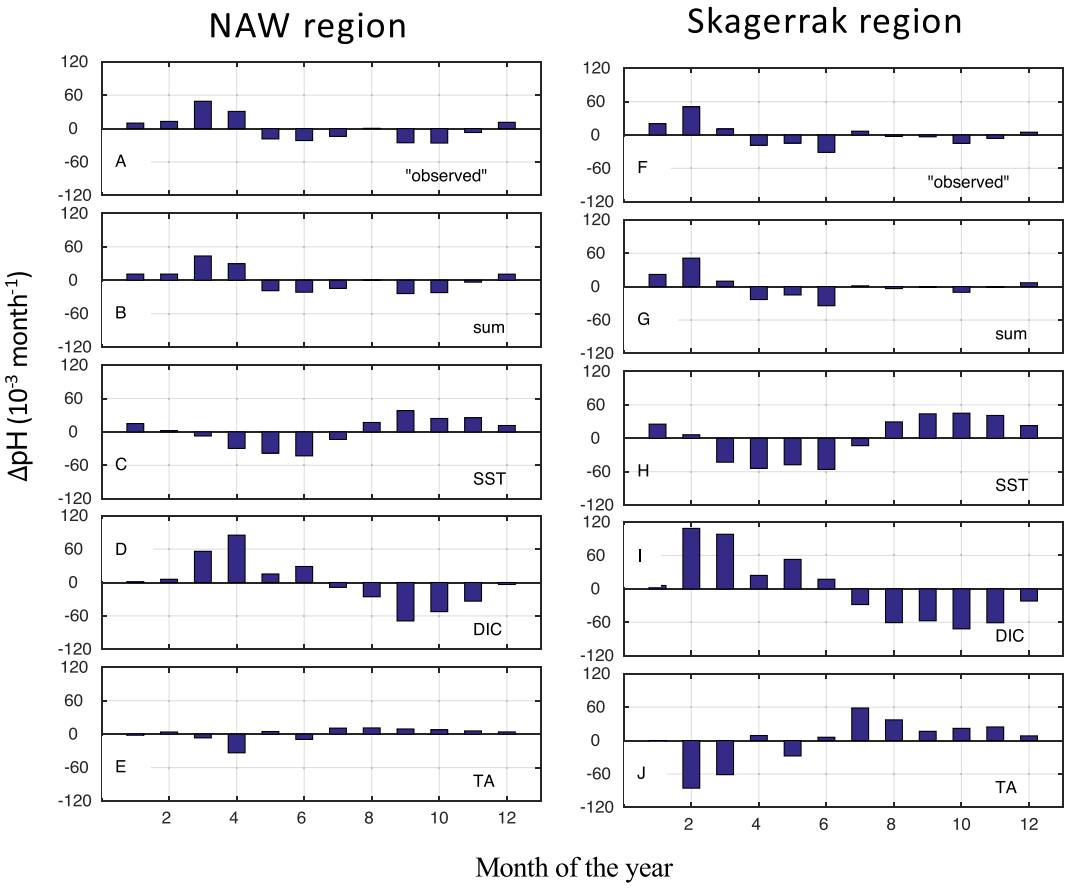

Figure 3. Monthly pH changes (ΔpH) as observed (a, f) and expected due to sum of all derivers (b, g), SST changes (c, h), DIC changes (d, i), and by TA changes (e, j) in the North Atlantic Water region (left) and Skagerrak region (right). SST = sea surface temperature; DIC = dissolved inorganic carbon; TA = total alkalinity.

c, 2e, and 2f). This despite the fact that the seasonal changes in all these variables (pCO_2, pH, and Ω_{ar}) are produced by the interplay of the phytoplankton spring bloom, summer warming/winter cooling, and freshwater input. The temperature sensitivity of Ω_{ar} is smaller compared to that for pH and pCO_2, and Ω_{ar} reaches its minimum values (≈1.5) during winter (January–March) when both pH and SST are low.

The Skagerrak region is characterized by stronger seasonal variations with much stronger spring-summer warming and freshening and higher NPP than the NAW region. The stronger seasonality in SST and SSS also contributes to stronger seasonality in Ω_{ar} in the Skagerrak region while for pCO_2 and pH, the seasonality is comparatively uniform across the longitudinal transect.

The controls on the seasonal pCO_2 variability in the study area were investigated previously by Omar et al. (2010) using a method that quantifies the effect of driving processes (Olsen et al., 2008). They showed that pCO_2 in the northern North Sea is controlled by (in a decreasing order) mixing and biology, changes in SST, and air-sea CO_2 exchange. Here, we use a different decomposition method that quantifies the effect of driving variables (DIC, TA, SST, and SSS) on the monthly changes of observed pCO_2 and computed pH and Ω_{ar} to gain more insight into the parameters governing the seasonal variations and their relative importance. Further, since the controls of pCO_2 and pH are identical (below), in the following, we will only discuss decomposition results for pH and Ω_{ar}. Furthermore, in order to accommodate for the observed different water masses and seasonality (section 3.1), we analyze results for the NAW and Skagerrak regions separately.

For pH, we used the decomposition method described in Lauvset et al. (2015) to quantify the importance of different drivers. This method first estimates the monthly pCO_2 changes expected from changes in SST, SSS, DIC, and TA as well as their sum. It then converts the pCO_2 changes to pH. The results are shown in

Figures 3a–3j (SSS had a negligible effect on the seasonal pH variations and is therefore not shown). For the NAW region, DIC is the most important driver followed by SST and TA (Figures 3c–3e). The seasonal variability in DIC causes pH to increase during the first half of the year and to decrease during the second half of the year, whereas the SST effect primarily opposes that of DIC, that is, it causes pH to decrease during February–July and to increase during August–January. The influence of DIC during spring and fall outweighs the effect of SST, and pH increases due to decreasing SST in December–February and due to decreasing DIC in March–April. The increased importance of TA during spring and fall is evident from Figures 3e and 3j. During spring, larger TA decrease is produced by increased freshwater input from the Baltic and Scandinavian rivers. During fall, larger TA increase is produced by S increase (due to the erosion of the mixed layer). Both these effects are more pronounced in the Skagerrak where changes of freshwater input are biggest. The effects of SST and TA combined are nearly equal to but opposite to that of DIC (Figures 3c–3e). As a result, the sum of all computed effects is small (<0.05 pH units). Note also that the decomposition model is able to account for the observed seasonal changes, that is, the sum of the computed effects compares well with the observed amplitudes (Figure 3a).

The seasonal dynamics and controls on pH in the Skagerrak region are similar to those in the NAW region (described above), but the effect of SST, DIC, and TA on the monthly pH changes are enhanced in the Skagerrak region (Figures 3h–3j). This especially holds for TA, which has an up to five times stronger influence on pH in the Skagerrak region compared to the NAW region. Note also that the TA control is larger than that of SST during spring and fall seasons. Again, the effects of SST and TA combined are nearly equal to, but opposite to, that of DIC (Figures 3h–3j), and the sum of all effects is small (<0.06 pH units).

It must be noted that above quantified drivers of pCO_2 and pH also indicate the importance of different processes throughout the year. For instance, the strong DIC and SST controls during spring/summer confirm that photosynthesis, which takes up carbon from the surface water, is the dominant process followed by the effect of spring/summer warming, which has direct increasing/decreasing effect on pCO_2/pH, respectively. During fall, on the other hand, DIC and SST are dominant controls because upward mixing of colder CO_2-rich deeper water (e.g., Thomas et al., 2005) increases DIC while falling temperatures have direct decreasing/increasing effect on pCO_2/pH.

We decomposed the seasonal changes of Ω_{ar} according to:

$$d\Omega_{ar}/dt = \frac{d\Omega_{ar}}{dSST} SST_{slope} + \frac{d\Omega_{ar}}{dSSS} SSS_{slope} + \frac{d\Omega_{ar}}{dDIC} DIC_{slope} + \frac{d\Omega_{ar}}{dTA} TA_{slope} \quad (1)$$

where $d\Omega_{ar}/dDIC$ and $d\Omega_{ar}/dTA$ have been determined from the analytical expressions given by Egleston et al. (2010, see their Table 1), and $d\Omega_{ar}/dSST$ and $d\Omega_{ar}/dSSS$ have been estimated for the present data using the CO2SYS program (Lewis & Wallace, 1998). During these estimations, DIC and TA were held at their mean values, and either SST or SSS was varied between −2 and 25 °C or 30 and 36 °C, respectively. The values obtained from equation (1) are shown on Figure 4. The seasonal changes in DIC and TA are the most important drivers for changes in Ω_{ar} whereas the effects of variations of SST and SSS (not shown) on Ω_{ar} are negligible. This is in agreement with Omar et al. (2016), who analyzed data from the southwestern Norwegian coast using a different method and concluded that seasonal changes in DIC and TA are the most important drivers for changes in Ω_{ar}, and variations of SST and SSS are less relevant. Again, we note that the TA influence is enhanced in the Skagerrak region compared to the NAW region. We also note that the TA control outweighs that of DIC in July in the Skagerrak region (to be explained shortly). In both regions, Ω_{ar} increases between February and July primarily due to decreasing DIC driven by biological activity, while it decreases between September and December primarily due to increasing DIC driven by vertical mixing and respiration of organic matter. TA tends to have a decreasing effect on Ω_{ar} in the first half of the year due to decreasing TA that result from freshwater input throughout later winter (March) and midsummer (July). During the rest of the year, TA increases due to increasing SSS, and this has an increasing effect on Ω_{ar}. This also demonstrates how S variations indirectly impact Ω_{ar} through TA and DIC both of which directly covary with SSS. The effect of this indirect SSS control (through TA and DIC) on Ω_{ar} partially cancels out because DIC and TA have opposing effects on Ω_{ar}. Firstly, the sensitivity of Ω_{ar} to DIC and TA changes are opposite and nearly equal (i.e., $d\Omega_{ar}/dDIC$ and $d\Omega_{ar}/dTA$ in equiation (1) have equal magnitudes and opposite signs). Secondly, for any given change in SSS, the resulting TA change is about 30% larger than

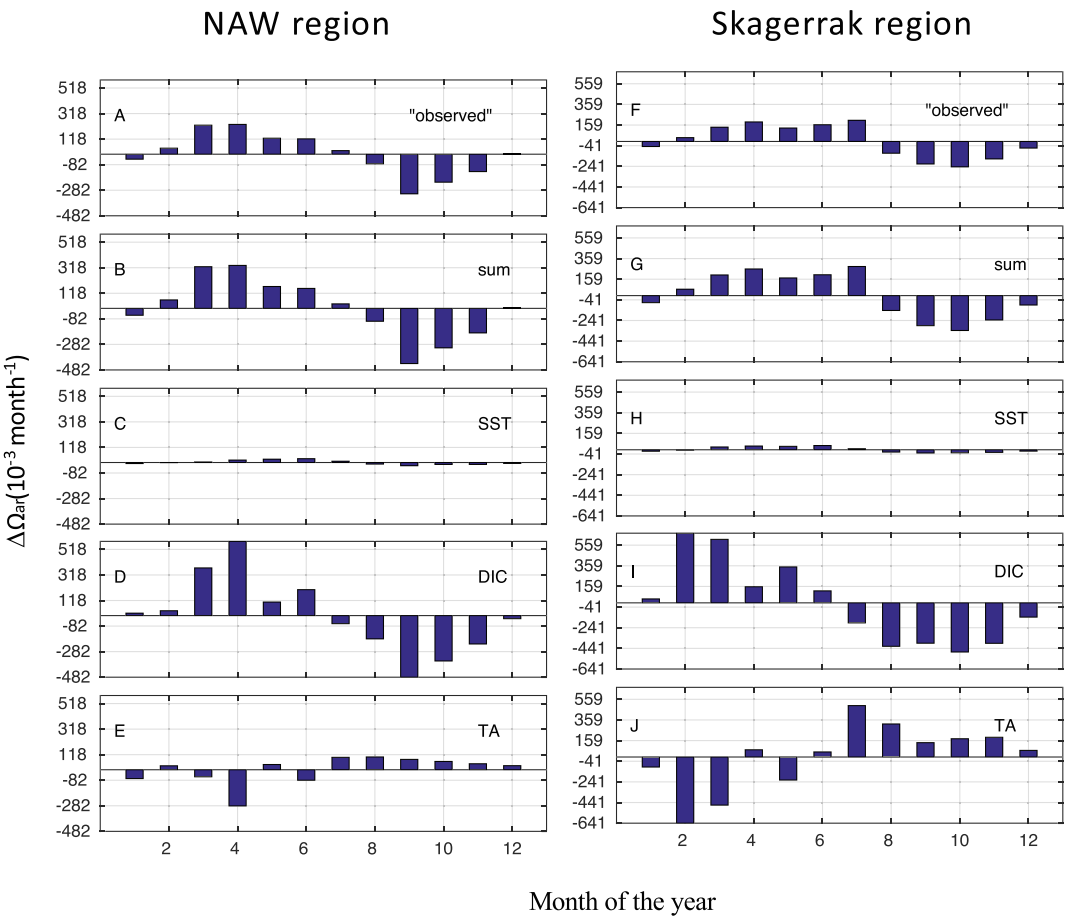

Figure 4. As in Figure 3 but for monthly Ω_{ar} changes. Note different scales in *y* axis. SST = sea surface temperature; DIC = dissolved inorganic carbon; TA = total alkalinity.

the corresponding DIC change so that a net impact on Ω_{ar} would be expected. However, monthly DIC changes result from several processes and are almost always larger than TA changes. Hence, the indirect net effect from SSS changes (through TA) is outweighed by larger DIC influence from processes other than SSS changes (compare Figures 4d and 4e and 4i and 4j). An exception is in July when both DIC and TA increase, but disproportionally; TA increases due to increasing S, but DIC does not keep up probably due to biological uptake neutralizing the effect of increasing SSS (Figure S4). Hence, Ω_{ar} increases due to increasing TA in July. This is particularly clear for the Skagerrak region (Figures 4i and 4j). In short, DIC is the primary driver of the seasonal changes in Ω_{ar}, but TA changes have secondary effects that reduce the amplitude of the seasonal Ω_{ar} changes produced by DIC changes except in July when TA exerts the strongest control on Ω_{ar} (see Figure 4 and Figure S4).

3.3. Interannual Variations, Trends, and Controls

The interannual variations were determined as percentage standard deviations associated with each monthly mean over the study period; 2004–2015 for the NAW region and 2004–2012 for the Skagerrak. The reason for the different lengths is due to the fact that TA measurements of the cruise in 2015 were available only for the NAW region. Thus, for the Skagerrak region, complete CO_2-system parameters could not be computed from the underway data for the years 2013–2015. The possible effect of these different time series lengths on the computed trends is discussed at the end of the section. The monthly means were deseasonalized by subtracting the long-term mean of the respective month (e.g., Tjiputra et al., 2014) before the computation of the standard deviations. The computed interannual variations are generally between 3–15% for pCO_2 and Ω_{ar} and less than 10% for all other parameters (Figure 5) with the exception of late winter/spring SSTs in the

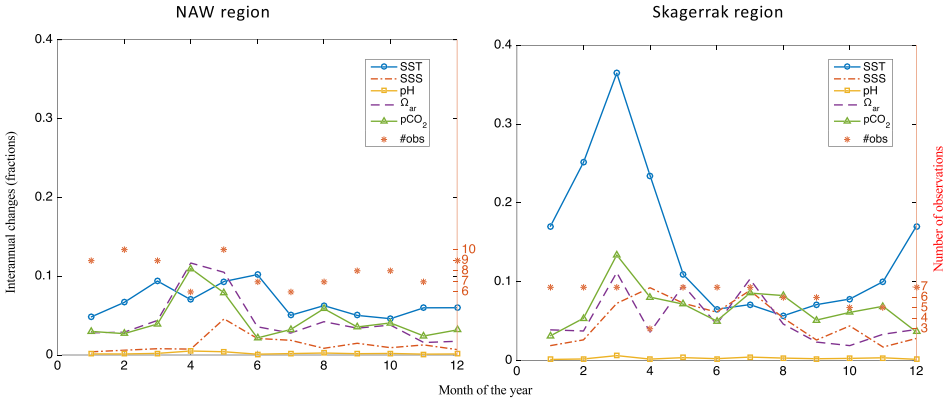

Figure 5. Interannual changes (standard deviations relative to the long-term monthly averages) in SST, SSS, pCO_2, pH, and Ω_{ar} as a function of month of the year. Also shown are the number of monthly averages available in each month for all the above variables in the observation period (2004–2015 for North Atlantic Water region and 2004–2012 for the Skagerrak region). SSS = sea surface salinity; SST = sea surface temperature

Skagerrak, which show higher interannual variations of 15–35%. Generally, the Skagerrak region shows higher interannual variations except during spring when pCO_2, pH, and Ω_{ar} variations are 1.5–3 times larger in the NAW region. The lowest relative interannual changes are observed for pH (0.3–0.4%) and SSS (<5%) in the NAW region. Interannual SSS changes in the Skagerrak region (2–10%) are much larger than those for the NAW region. For all variables (except SST in the Skagerrak), interannual variability is lowest during winter and fall and highest during spring, a finding that is in good agreement with the results of Omar et al. (2010). Winter time pCO_2 interannual changes were around 3% both in the NAW and Skagerrak regions, and the decomposition analyses we have performed (not shown) revealed that the interannual changes in pCO_2, pH, and Ω_{ar} have the same drivers (in parameter and magnitude) as the seasonal changes. This means that interannual variations are primarily driven by DIC changes counteracted by the combined effects of TA and SST changes, while SSS has the least importance. Furthermore, interannual changes are highest during spring (April and May) mainly due to enhanced DIC and TA changes that are slightly phase shifted to each other, that is, counteracting each other to a smaller degree compared to the winter situation.

For the determination of the trends, we used winter (December–February) data for the NAW region and (December–January) data for the Skagerrak region. We choose not to include March (and February for the Skagerrak) because significant primary production takes place in these months, especially in the Skagerrak region (Figure 2d). The computed trends superimposed on the long-term wintertime mean values (2003–2015 for the NAW region and 2003–2012 for the Skagerrak region) are shown in Figure 6. The superposition of the long-term mean values was convenient in order to give an idea about the temporal development of mean values in the study area. Also, note that data for winter 2003 were actually acquired in January/February 2004, that is, winter 2003 means winter 2003/2004 and so on.

Statistically significant long-term trends, that is, with $p < 0.05$ are evident in the NAW region for pCO_2, pH, and Ω_{ar} (Figures 6a–6c and Table 2). The observed trends of increasing pCO_2 and decreasing pH and Ω_{ar} are consistent with the effects of anthropogenic CO_2 uptake by the surface ocean leading to OA. The trends are also within the range of the global atmospheric pCO_2 growth rate (2.0 μatm/year), and the OA expected from it (0.0018 ± 0.0002 pH unit per year (e.g., Lauvset et al., 2015), considering the uncertainties. Furthermore, decomposing the drivers of the observed trends indicates that the decreasing pH trend in the NAW originates almost entirely from increasing DIC while SSS has negligible influence (Figures 7a and 7b). TA and SST do have significant effects in driving the pH trend, but these effects are much smaller than that of DIC (Figures 7a and 7b). The same drivers control the pCO_2 growth rate with impact strengths equal to those shown for pH but with opposite sign. Similarly, the decomposition of the Ω_{ar} trends shows that DIC and TA are the most important drivers and the effect of TA is much smaller than that of DIC (Figures 7c and 7d). It must be emphasized that the sensitivity of Ω_{ar} to changes in SST, SSS, DIC, and TA, that is, the coefficients of equation (1) is of the same magnitude, but the trend in Ω_{ar} driven by DIC dominates, because the

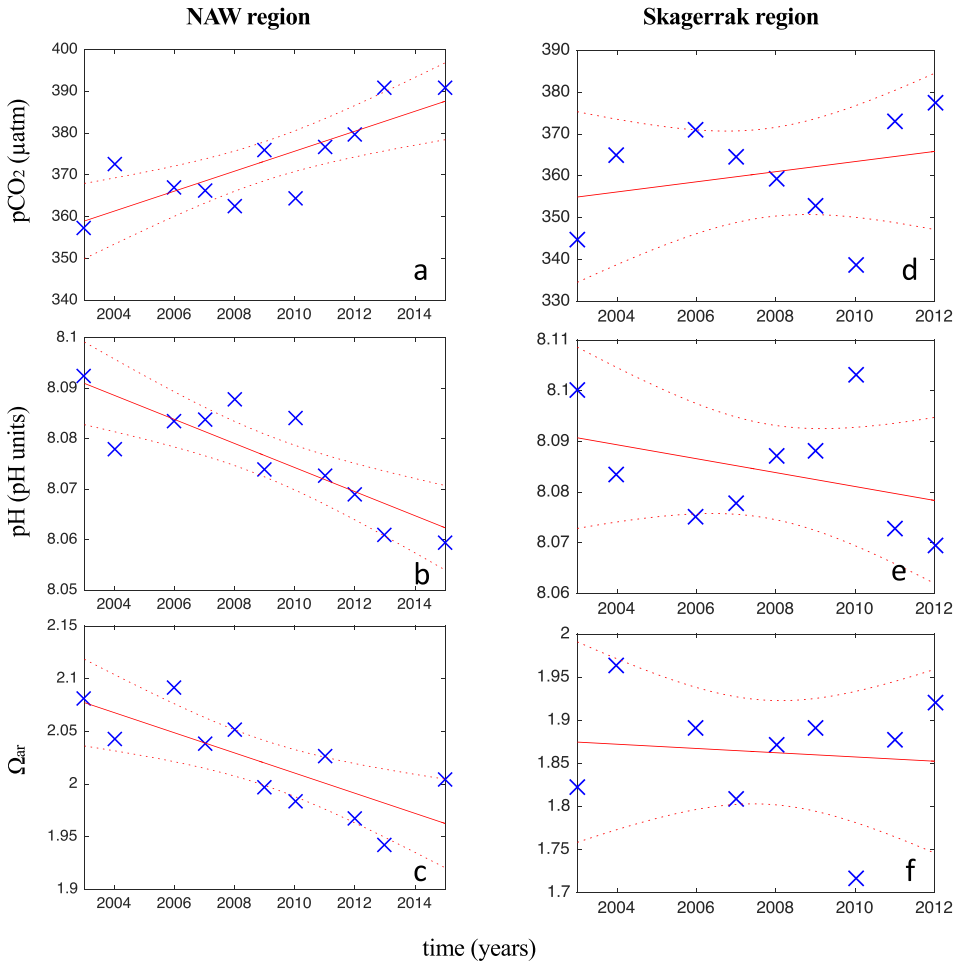

Figure 6. Long-term trends in winter-time pCO_2 (a and d), pH (b and e), and Ω_{ar} (c and e) superimposed on the long-term winter mean values as a function of time (years). For the computation of the trends monthly means were deseasonalized by subtracting the long-term mean of the respective months (see section 3.3 of the main text). Also shown are the best fit (solid) and 95% confidence lines (dotted). Note the different ranges in both axes. NAW = North Atlantic Water.

trend in DIC (1.2 ± 0.3 µmol/kg/year) is numerically up to an order of magnitude larger than those in SST, SSS, and TA (Table 2).

The pCO_2 trend in the NAW region is in general agreement with that reported for the adjacent subpolar North Atlantic where Lauvset and Gruber (2014) reported a seawater CO_2 fugacity (fCO_2) and pH trends of 2.0 ± 0.38 µatm/year and −0.0022 ± 0.0004 pH units per year, respectively, for the period 1981–2007. Newer wintertime fCO_2 data collected from the subpolar North Atlantic aboard Nuka in 2004–2016 show fCO_2 growth rates that increase from the Irminger Sea in the west (1.96 ± 0.27 µatm/year) to the Faeroe Bank Channel in the east (2.27 ± 0.14 µatm/year), mainly driven by DIC (Fröb et al., 2018). Thus, the computed wintertime pCO_2 trend in the NAW region is similar to that observed in the adjacent open ocean. It should be noted, however, that the summer trend (or annual mean trend) in the NAW region may be different from the value determined in this study.

Laruelle et al. (2018) summarized two main mechanisms which have been described in the literature to explain the evolution of the continental shelf CO_2 sink. One mechanism relies on the timescales of air–water and shelf–open ocean exchanges of CO_2, the other on the stimulation of the biological pump. According to the former mechanism, if shelf–open ocean exchanges of CO_2 are unable to keep up with the increasing air–sea flux of anthropogenic CO_2, CO_2 may accumulate in shelf waters so that seawater pCO_2 increase follows the atmosphere due to this bottleneck in offshore transport. In that respect, the fact that the pCO_2 trend in

Table 2
Computed Trends in Wintertime SST, SSS, pCO_2, pH, and Ω_{ar} in 2004–2015 for the North Atlantic Water and for the Skagerrak Regions of the North Sea

Region	Parameter (unit)	Trend	Standard error (±)	R^2	p	#Obs.
North Atlantic Water	SST (°C/year)	−0.004	0.040	<0.1	0.92	11
	SSS ($year^{-1}$)	0.007	0.011	<0.1	0.57	11
	pCO_2 ($\mu atm/year^{-1}$)	2.39	0.58	0.66	<0.01	11
	pH ($year^{-1}$)	−0.0024	0.001	0.70	<0.01	11
	Ω_{ar} ($year^{-1}$)	−0.010	0.003	0.59	<0.01	11
	DIC ($\mu mol \cdot kg^{-1} \cdot year^{-1}$)	1.2	0.3	0.59	<0.01	11
	TA ($\mu mol \cdot kg^{-1} \cdot year^{-1}$)	0.1	0.3	<0.1	0.68	11
Skagerrak	SST (°C/year)	−0.026	0.153	<0.1	0.87	9
	SSS ($year^{-1}$)	0.037	0.099	<0.1	0.72	9
	pCO_2 ($\mu atm/year^{-1}$)	1.2122	1.5440	<0.1	0.46	9
	pH ($year^{-1}$)	−0.0014	0.0014	0.1	0.34	9
	Ω_{ar} ($year^{-1}$)	−0.0025	0.0088	<0.1	0.79	9
	DIC ($\mu mol \cdot kg^{-1} \cdot year^{-1}$)	1.3	1.6	<0.1	0.44	9
	TA ($\mu mol \cdot kg^{-1} \cdot year^{-1}$)	1.0	2.4	<0.1	0.68	9

Note. The trends are computed from December–February data for the North Atlantic Water region and from December–January data for the Skagerrak (see section 3.3 of the main text). DIC = dissolved inorganic carbon; pCO_2 = carbon dioxide partial pressure; SSS = sea surface salinity; SST = sea surface temperature; TA = total alkalinity; Ω_{ar} = aragonite saturation state.

the NAW region closely tracks the atmosphere indicates that the accumulation of anthropogenic CO_2 in this region occurs faster than it is being transported to the open ocean.

In the Skagerrak region, the long-term trends are weaker (Table 2, second part) and statistically insignificant ($R^2 < 0.2$ and $p > 0.3$). Therefore, it is fair to report that the Skagerrak region does not show any clear trends in wintertime pCO_2 and OA variables during the period 2004–2012. Nevertheless, the decomposition shows that TA and DIC are the major drivers of the annual changes, and they have opposite and equal effects on pH (Figure 7b). Furthermore, SSS and SST have decreasing effects on pH, but these are much smaller effects compared to the controls of TA and DIC (Figure 7b). We also note that the magnitudes of drivers are larger in the Skagerrak compared to the NAW region. This is especially true for SSS and TA drivers which are six and nine times stronger than those in NAW. In short, SSS and TA increases counteract the effect of DIC increase, and the overall trends are weaker in the Skagerrak compared to the NAW region.

The reason for the absence of statistically significant trends in the Skagerrak region is not the main subject of this study and will not be treated comprehensively. However, few plausible explanations are discussed in the following. First, we analyzed shorter time series for the Skagerrak region since we focused on the computed OA parameters that were available only until 2012 (cruise TA data were available only until 2011 for this region, see Figure 1). However, this is not the sole reason for absence of significant trends in the Skagerrak region because the NAW region presents more clear trends even if time series of equal lengths are analyzed for the two regions. For instance, if the time series of the NAW region is shortened to 8 years, the resulting trends would still have p-values ranging from 0.03 to 0.09 which are much lower than those for the Skagerrak region (Table 2). On the other hand, including all wintertime pCO_2 data measured in the Skagerrak region between 2004 and 2015 result in a pCO_2 trend that is statistically insignificant ($R^2 < 0.3$ and $p = 0.07$) and highly uncertain (2.4 ± 1.2 $\mu atm/year$).

Second, both DIC and TA in the Skagerrak region showed increasing trends (although the TA trend was not statistically significant, $p = 0.68$), but the effect of the increasing DIC on pCO_2 growth and OA parameters has been effectively counteracted by the effect of increasing TA (Figure 7b). Thus it seems that the oceanic pCO_2 growth and OA trend expected in this region due to the increased atmospheric CO_2 are counteracted by TA increase. In fact, Wesslander et al. (2010) reported that TA in both Kattegat and the central Baltic Sea has increased over the 1993–2009 period probably due to internal change in the Baltic Sea circulation. It is therefore conceivable that increased TA in the Baltic outflow has affected the Skagerrak region as well. As mentioned above, the current TA data obtained between 2005 and 2012 also indicate an increasing trend

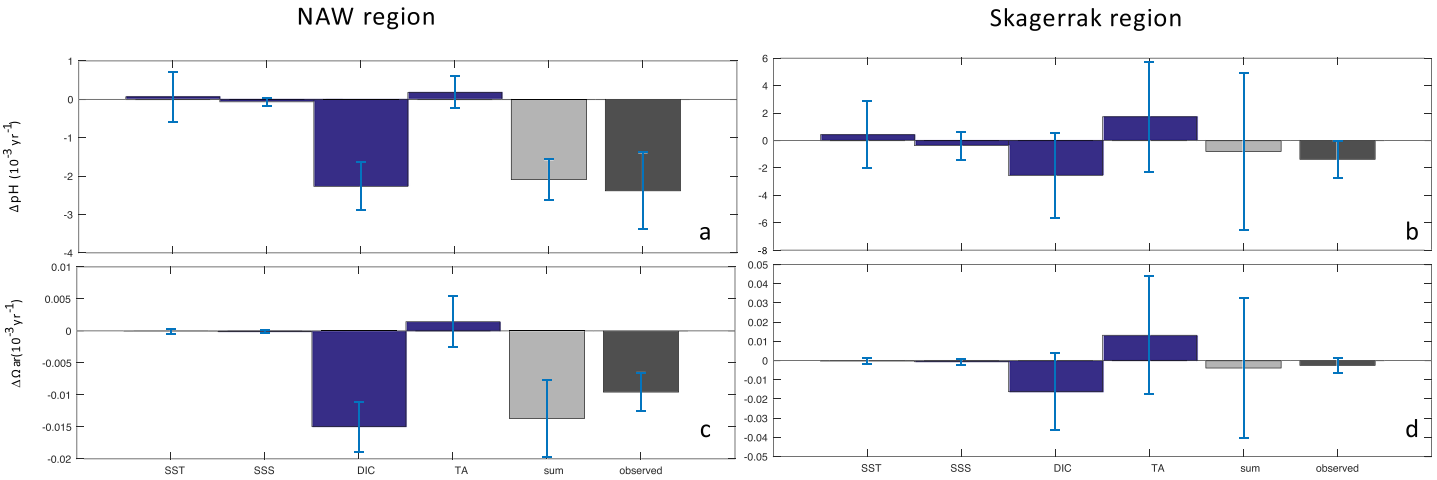

Figure 7. Long-term pH (a) and Ω_{ar} (c) annual changes as observed (black bars) and as expected due to sum of all drivers (gray bars), SST changes, DIC changes, and by TA changes in the NAW region. (b) and (d) as above but for the Skagerrak region. Note that the scales in the *y* axis are different on the Ω_{ar} panels (c and d). The error bars indicate the uncertainties associated with the estimated changes. The individual errors are calculated by using the errors of the respective trends (see Table 2) and the total error was calculated as the square root of the sum of squares of the individual errors. NAW = North Atlantic Water; SST = sea surface temperature; DIC = dissolved inorganic carbon; TA = total alkalinity.

in the Skagerrak region. However, this TA trend must be interpreted with care because it is not statistically significant, and the TA data have been estimated from S. This highlights the necessity of a measured TA time series in the area.

A third possible explanation is that the maximal pCO_2 (and lowest pH) values are controlled by different processes in the two regions. In the NAW region, the highest pCO_2 values are controlled by upward mixing of CO_2-rich deep water and uptake of atmospheric CO_2. This brings the wintertime surface seawater to near equilibration with the atmospheric CO_2 level (e.g., Omar et al., 2010; Thomas et al., 2005). The December–January disequilibrium (seawater pCO_2–atmospheric pCO_2) in the NAW region ranged between 2 and −27 μatm with a mean value of -12 ± 8 μatm. In the Skagerrak region, on the other hand, the average December–January pCO_2 disequilibrium was larger (-21 ± 8 μatm) compared to the NAW, ranging between −6 and −35 μatm. The larger disequilibrium in the Skagerrak region was specially enhanced in 2004 and 2007–2009 (Figure S3) when winter pCO_2 values were on average 27 μatm lower than atmospheric pCO_2. This indicates that wintertime pCO_2 in the Skagerrak region is probably governed by the combination of biological activity, sediment water interaction, and mixing (both lateral and vertical). In other words, our assumption that "the influence of biological activity is negligible" during wintertime is probably not fully met in the Skagerrak region. In particular, two ways biological activity in wintertime can conceal trends are either by introducing elevated interannual variability or by including trends that counteract the effect of C_{ant}. The latter is more plausible since wintertime interannual variability is only slightly higher in the Skagerrak compared to the NAW region (Figure 5). One particular mechanism, which involves all the aforementioned processes and which has been reported for the southern North Sea (Burt et al., 2016) is the denitrification of the allochthonous nitrate in near-coastal regions, which creates an increase in the standing stock of TA, strongly buffering the effect of OA (e.g., Borges & Gypens, 2010). However, denitrification is not a particularly dominant process of organic matter degradation in the Skagerrak area (Rysgaard et al., 2001).

In any case, a more complete understanding of the absence of statistically significant trends in the Skagerrak region is important since it is a prerequisite for predicting the future development of CO_2 sink and OA in the area. A first step toward this goal is to investigate the relative importance of the solubility and biological pumps in the development of the CO_2 system in the Skagerrak on decadal time scales. The resolution of this issue requires not only a sustained measurement program, but also measurements that integrate physical, biological, and chemical data sets. This needs to be taken into account by monitoring programs such as the Ocean Acidification monitoring project, funded by the Norwegian Environmental Agency, which

covers areas including the Skagerrak region. In the 2016 report from this monitoring project, Chierichi et al. (2017) analyzed 5 years of data of the CO_2 system, temperature, and S, obtained from repeated stations in the Skagerrak. They found significant pH and Ω_{ar} trends only in the deepest part of the water column (below 600 m). In the surface water, on the other hand, no statistically significant trends were observed between 2011 and 2016 in agreement with our results. Furthermore, Chierichi et al. (2017) concluded that longer time series were needed to investigate the long-term trends in the area, and they recommended more comprehensive monitoring, that is, include integrated measurements and studies of primary production, ocean physics, freshwater supplies, and land-sea exchanges. Based on the results of our analyses, we support these recommendations and suggest that in addition to time series of sufficient length, the measured variables and analyses methods also need to be widened. This will enable accounting for the effects of physical and biological process on the long-term development of CO_2-system parameters in the Skagerrak region. Furthermore, such an extended data set would give us opportunity to determine trends for all seasons and not only during winter.

3.4. Conclusions and Further Comments

A new, decade-long, time series enabled us to investigate the variability in surface seawater pCO_2 and acidification parameters in the northern North Sea (2004–2015) on seasonal, interannual, and decadal time scales. The area is found to be a year-round CO_2 sink and subject to strong seasonal changes and intermediate interannual variations. Regarding the decadal development of pCO_2 and OA parameters during winter (the season with minimal interannual variability and biological activity), the study area shows a clear west-east division in accordance with the well-known high spatial heterogeneity in shelf regions. In the western part (the NAW region), wintertime trends are statistically significant and similar to what is expected from atmospheric CO_2 increase and observed in the adjacent open-ocean region. This indicates that the surface waters in this shelf region fully equilibrate with atmospheric CO_2 perturbation before they are transported to the open ocean.

In the eastern parts (the Skagerrak region), wintertime trends are weaker and statistically insignificant. The exact reasons for this are not known, but interannual variability, which could entail longer times of emergence for trends, seem to play a minor role. It is thus likely that compensating trends (e.g., in biological activity, sediment water interaction, mixing, circulation, etc.) are concealing the anthropogenic trends in CO_2-system variables in the Skagerrak region. In order to understand and disentangle these trends for all seasons of the year, there is a need for sustained measurements incorporating physical, biological, and chemical parameters.

Acknowledgments
This work has received funding from the European Union's Horizon 2020 research and innovation program (654462), the Research Council of Norway (245972), and the Norwegian Environment Agency (258608). We are grateful for the technical assistance provided by Tor de Lange, Kristin Jackson, and Sigve Naustdal. We are also grateful for two anonymous referees whose comments and suggestions improved the manuscript. This work would not have been possible without the generosity and help of the liner company Royal Arctic Line AS and the captains and crew of MS Nuka Arctica. We thank INSU for support to SNO SSS and LEGOS/OMP for validation and archiving of the data of the thermosalinograph. Helmuth Thomas acknowledges support by the German Academic Exchange Service DAAD (57429828) from funds of the German Federal Ministry of Education and Research (BMBF). Data used in this study are accessible at SOCAT (https://www.nodc.noaa.gov/ocads/oceans/glodap/GlopDV.htmlhttp://www.socat.info/), GLODAP v2 (https://www.nodc.noaa.gov/ocads/oceans/glodap/GlopDV.html), and the Ocean Productivity website http://orca.science.oregonstate.edu/1080.by.2160.monthly.xyz.vgpm.m.chl.m.sst.php .

References

Alory, G., Delcroix, T., Téchiné, P., Diverrés, D., Varillon, D., Cravatte, S., et al. (2015). The French contribution to the voluntary observing ships network of sea surface salinity. *Deep Sea Research Part I: Oceanographic Research Papers*, *105*, 1–18. https://doi.org/10.1016/j.dsr.2015.08.005

Bakker, D. C. E., Pfeil, B., Smith, K., Hankin, S., Olsen, A., Alin, S. R., et al. (2014). An update to the Surface Ocean CO2 Atlas (SOCAT version 2). *Earth System Science Data*, *6*(1), 69–90. https://doi.org/10.5194/essd-6-69-2014

Bates, N. R., Asto, Y., Church, M., Currie, K., Dore, J., González-Dávila, M., et al. (2014). A time-series view of changing ocean chemistry due to ocean uptake of anthropogenic CO2 and ocean acidification. *Oceanography*, *27*(1), 126–141. https://doi.org/10.5670/oceanog.2014.16

Behrenfeld, M. J., & Falkowski, P. G. (1997). Photosynthetic rates derived from satellite-based chlorophyll concentration. *Limnology and Oceanography*, *42*, 1–20.

Borges, A. V., & Gypens, N. (2010). Carbonate chemistry responds more strongly to eutrophication than ocean acidification in the coastal zone. *Limnology and Oceanography*, *55*(1), 346–353. https://doi.org/10.4319/lo.2010.55.1.0346

Bousquet, P., Gaudry, A., Ciais, P., Kazan, V., Monfray, P., Simmonds, P. G., et al. (1996). Atmospheric CO2 concentration variations recorded at Mace Head, Ireland, from 1992 to 1994. *Physics and Chemistry of the Earth*, *21*(5-6), 477–481. https://doi.org/10.1016/S0079-1946(97)81145-7

Bozec, Y., Thomas, H., Elkalay, K., & de Baar, H. J. W. (2005). The continental shelf pump for CO2 in the North Sea—Evidence from summer observations. *Marine Chemistry*, *93*(2-4), 131–147. https://doi.org/10.1016/j.marchem.2004.07.006

Bozec, Y., Thomas, H., Schiettecatte, L.-S., Borges, A. V., Elkalay, K., & de Baar, H. J. W. (2006). Assessment of the processes controlling the seasonal variations of dissolved inorganic carbon in the North Sea. *Limnology and Oceanography*, *51*(6), 2746–2762. https://doi.org/10.4319/lo.2006.51.6.2746

Burt, W. J., Thomas, H., Hagens, M., Pätsch, J., Clargo, N. M., Salt, L. A., et al. (2016). Carbon sources in the North Sea evaluated by means of radium and stable carbon isotope tracers. *Limnology and Oceanography*, *61*(2), 666–683. https://doi.org/10.1002/lno.10243

Cai, W. J., Huang, W. J., Luther, G. W., Pierrot, D., Li, M., Testa, J., et al. (2017). Redox reactions and weak buffering capacity lead to acidification in the Chesapeake Bay. *Nature Communications*, *8*(1), 369. https://doi.org/10.1038/s41467-017-00417-7

Chierichi, M., Skjelvan, I., Norli, M., Jones, E., Børsheim, K. Y., Lauvset, S. K., et al.. (2017). Overvåking av havforsuring i norske farvann i 2016, Rapport, Miljødirektoratet, M-776. (in Norwegian).

Clargo, N. M., Salt, L. A., Thomas, H., & de Baar, H. J. W. (2015). Rapid increase of observed DIC and pCO2 in the surface waters of the North Sea in the 2001–2011 decade ascribed to climate change superimposed by biological processes. *Marine Chemistry*, *177*, 566–581. https://doi.org/10.1016/j.marchem.2015.08.010

Dickson, A. G. (1990). Standard potential of the reaction: AgCl(s) + 1/2H2(g) = Ag(s) + Cl (aq), and the standard acidity constant of the ion HSO4—In synthetic seawater from 273.15 to 318.15 K. *The Journal of Chemical Thermodynamics*, *22*(2), 113–127. https://doi.org/10.1016/0021-9614(90)90074-Z

Dickson, A. G. (2010). The carbon dioxide system in seawater: Equilibrium chemistry and measurements. In U. Riebesell, V. J. Fabry, L. Hansson, & J.-P. Gattuso (Eds.), *Guide to best practices for ocean acidification research and data reporting* (Chap. 1, pp. 17–40). Luxembourg: Publications Office of the European Union.

Egleston, E. S., Sabine, C. L., & Morel, F. M. M. (2010). Revelle revisited: Buffer factors that quantify the response of ocean chemistry to changes in DIC and alkalinity. *Global Biogeochemical Cycles*, *24*, GB1002. https://doi.org/10.1029/2008GB003407

Frankignoulle, M., & Borges, A. V. (2001). The European continental shelf as a significant sink for atmospheric carbon dioxide. *Global Biogeochemical Cycles*, *15*, 569–576. https://doi.org/10.1029/2000GB001307

Fröb, F., Olsen, A., Becker, M., Chafik, L., Johannessen, T., Reverdin, G., & Omar, A. (2019). Wintertime fCO_2 variability in the subpolar North Atlantic since 2004. *Geophysical Research Letters*, *6*. https://doi.org/10.1029/2018GL080554

Johnson, K. M., Wills, K. D., Butler, D. B., Johnson, W. K., & Wong, C. S. (1993). Coulometric total carbon dioxide analysis for marine studies: Maximizing the performance of an automated gas extraction system and coulometric detector. *Marine Chemistry*, *44*(2-4), 167–187. https://doi.org/10.1016/0304-4203(93)90201-X

Kroeker, K. J., Kordas, R. L., Crim, R. N., Hendriks, I. E., Ramajo, L., Singh, G. G., et al. (2013). Impacts of ocean acidification on marine organisms: Quantifying sensitivities and interaction with warming. *Global Change Biology*, *19*(6), 1884–1896. https://doi.org/10.1111/gcb.12179

Laruelle, G. G., Cai, W. J., Hu, X., Gruber, N., Mackenzie, F. T., & Regnier, P. (2018). Continental shelves as a variable but increasing global sink for atmospheric carbon dioxide. *Nature Communications*, *9*(1), 11. https://hdl.handle.net/10.1038/s41467-017-02738-z

Lauvset, S., Gruber, N., Landschützer, P., Olsen, A., & Tjiputra, J. (2015). Trends and drivers in global surface ocean pH over the past 3 decades. *Biogeosciences*, *12*(5), 1285–1298. https://doi.org/10.5194/bg-12-1285

Lauvset, S. K., & Gruber, N. (2014). Long-term trends in surface ocean pH in the North Atlantic. *Marine Chemistry*, *162*, 71–76. https://doi.org/10.1016/j.marchem.2014.03.009

Lee, A. J. (1980). North Sea: Physical Oceanography, The north-west European shelf seas the seabed and the sea in motion II. Physical and Chemical Oceanography. In F. T. Banner, M. B. Collins, & K. S. Massie (Eds.), *Elsevier Oceanography Series, 24B* (pp. 467–493). Amsterdam: Elsevier.

Lewis, E., & Wallace, D. W. R. (1998). Program developed for CO2 system calculations, ORNL/CDIAC-105. Carbon Dioxide Information Analysis Center, Oak Ridge National Laboratory, U.S. Department of Energy.

Millero, F. J., Graham, T. B., Huang, F., Bustos-Serrano, H., & Pierrot, D. (2006). Dissociation constants of carbonic acid in seawater as a function of salinity and temperature. *Marine Chemistry*, *100*(1-2), 80–94. https://doi.org/10.1016/j.marchem.2005.12.001

Moll, A. (1997). Modelling primary production in the North Sea. *Oceanography*, *10*(1), 24–26. https://doi.org/10.5670/oceanog.1997.41

Nondal, G., Bellerby, R. G. J., Olsen, A., Johannessen, T., & Olafsson, J. (2009). Optimal evaluation of the surface ocean CO2 system in the northern North Atlantic using data from voluntary observing ships. *Limnology and Oceanography: Methods*, *7*, 109–118.

Olsen, A., Brown, K., Chierici, M., Johannessen, T., & Neill, G. C. (2008). Sea-surface CO2 fugacity in the subpolar North Atlantic. *Biogeosciences*, *5*(2), 535–547. https://doi.org/10.5194/bg-5-535-2008

Olsen, A., Key, R. M., van Heuven, S., Lauvset, S. K., Velo, A., Lin, X., et al. (2016). The Global Ocean Data Analysis Project version 2 (GLODAPv2)—An internally consistent data product for the world ocean. *Earth System Science Data*, *8*(2), 297–323. https://doi.org/10.5194/essd-8-297

Olsson, K., & Anderson, L. G. (1997). Input and biogeochemical transformation of dissolved carbon in the Siberian shelf seas. *Continental Shelf Research*, *17*(7), 819–833. https://doi.org/10.1016/S0278-4343(96)00059-3

Omar, A., Olsen, A., Johannessen, T., Hoppema, M., Thomas, H., & Borges, A. (2010). Spatiotemporal variations of fCO2 in the North Sea. *Ocean Science*, *6*(1), 77–89. https://doi.org/10.5194/os-6-77-2010

Omar, A. M., Skjelvan, I., Erga, S. R., & Olsen, A. (2016). Aragonite saturation states and pH in western Norwegian fjords: Seasonal cycles and controlling factors, 2005–2009. *Ocean Science*, *12*(4), 937–951. https://doi.org/10.5194/os-12-937-2016

Otto, L., Zimmerman, J. T. F., Furnes, K., Mork, M., Saetre, R., & Becker, G. (1990). Review of the physical oceanography of the North Sea. *Netherlands Journal of Sea Research*, *26*(2-4), 161–238. https://doi.org/10.1016/0077-7579(90)90091-T

Pierrot, D., Neill, C., Sullivan, K., Castle, R., Wanninkhof, R., Luger, H., et al. (2009). Recommendations for autonomous underway pCO2 measuring systems and data-reduction routines. *Deep Sea Research, Part II*, *56*(8-10), 512–522. https://doi.org/10.1016/j.dsr2.2008.12.005

Provoost, P., van Heuven, S., Soetaert, K., Laane, R. W. P. M., & Middelburg, J. J. (2010). Seasonal and long-term changes in pH in the Dutch coastal zone. *Biogeosciences*, *7*(11), 3869–3878. https://doi.org/10.5194/bg-7-3869-2010

Royal Society. (2005). Ocean acidification due to increasing atmospheric carbon dioxide. The Royal Society Policy Document 12/05. London. 68 pp.

Rysgaard, S., Fossing, H., & Jensen, M. M. (2001). Organic matter degradation through oxygen respiration, denitrification, and manganese, iron, and sulfate reduction in marine sediments (the Kattegat and the Skagerrak). *Ophelia*, *55*(2), 77–91. https://doi.org/10.1080/00785236.2001.10409475

Salt, L. A., Thomas, H., Bozec, Y., Borges, A. V., & de Baar, H. J. W. (2015). The internal consistency of the North Sea carbonate system. *Journal of Marine Systems*, *157*(2016), 52–64.

Salt, L. A., Thomas, H., Prowe, A. E. F., Borges, A. V., Bozec, Y., & de Baar, H. J. W. (2013). Variability of North Sea pH and CO2 in response to North Atlantic Oscillation forcing. *Journal of Geophysical Research: Biogeosciences*, *118*, 1584–1592. https://doi.org/10.1002/2013JG002306

Takahashi, T., Sutherland, S. C., Chipman, D. W., Goddard, J. G., Ho, C., Newberger, T., et al. (2014). Climatological distributions of pH, pCO(2), total CO2, alkalinity, and CaCO3 saturation in the global surface ocean, and temporal changes at selected locations. *Marine Chemistry*, *164*, 95–125. https://doi.org/10.1016/j.marchem.2014.06.004

Thomas, H. (2002). *Shipboard report of the RV Pelagia cruises 64PE184, 64PE187, 64PE190 and 64PE195*. Den Burg, Texel, Netherlands: Royal Netherlands Institute for Sea Research.

Thomas, H., Bozec, Y., Elkalay, K., & De Baar, H. (2004). Enhanced open ocean storage of CO2 from shelf sea pumping. *Science*, *304*(5673), 1005–1008. https://doi.org/10.1126/science.1095491

Thomas, H., Bozec, Y., Elkalay, K., De Baar, H. J. W., Borges, A. V., & Schiettecatte, L.-S. (2005). Controls of the surface water partial pressure of CO2 in the North Sea. *Biogeosciences*, *2*(4), 323–334. https://doi.org/10.5194/bg-2-323-2005

Thomas, H., Prowe, A. E. F., Van Heuven, S., Bozec, Y., De Baar, H. J. W., Schiettecatte, L.-S., et al. (2007). Rapid decline of the CO2 buffering capacity in the North Sea and implications for the North Atlantic Ocean. *Global Biogechemical Cycles*, *21*, GB4001. https://doi.org/10.1029/2006GB002825

Tilstone, G. H., Taylor, B., Blondeau-Patissier, D., Powell, T., Groom, S. B., Rees, A. P., & Lucas, M. (2015). Comparison of new and primary production models using SeaWiFS data in contrasting hydrographic zones of the northern North Atlantic. *Remote Sensing of Environment*, *156*, 473–489. https://doi.org/10.1016/j.rse.2014.10.013

Tjiputra, J., Olsen, A., Bopp, L., Lenton, A., Pfeil, B., Roy, T., et al. (2014). Long-term surface pCO_2 trends from observations and models. *Tellus B*, *66*(1). https://doi.org/10.3402/tellusb.v66.23083

van Heuven, S., Pierrot, D., Rae, J. W. B., Lewis, E., & Wallace, D. W. R. (2011). *MATLAB program developed for CO2 system calculations. ORNL/CDIAC-105b*. Oak Ridge, Tennessee, U.S.A: CDIAC, Oak Ridge National Laboratory, Department of Energy. https://doi.org/10.3334/CDIAC/otg.CO2SYS_MATLAB_v1.1

Wang, H., Hu, X., Cai, W.-J., & Sterba-Boatwright, B. (2017). Decadal fCO_2 trends in global ocean margins and adjacent boundary current-influenced areas. *Geophysical Research Letters*, *44*, 8962–8970. https://doi.org/10.1002/2017GL074724

Wesslander, K., Omstedt, A., & Schneider, B. (2010). Inter-annual and seasonal variations in the air–sea CO2 balance in the central Baltic Sea and the Kattegat. *Continental Shelf Research*, *30*(14), 1511–1521. https://doi.org/10.1016/j.csr.2010.05.014

Wootton, J. T., Pfister, C. A., & Forester, J. D. (2008). Dynamic patterns and ecological impacts of declining ocean pH in a high-resolution multi-year dataset. *PNAS*, *105*(48), 18848–18853. https://doi.org/10.1073/pnas.0810079105